Unexpected Nitrosyl-Group Bending in Six-Coordinate {M(NO)}^{6} σ-Bonded Aryl(iron) and -(ruthenium) Porphyrins

**George B. Richter-Addo,*,† Ralph A. Wheeler,*,† Christopher Adam Hixson,† Li Chen,†
Masood A. Khan,† Mary K. Ellison,‡ Charles E. Schulz,§ and W. Robert Scheidt*,‡**

*Contribution from Department of Chemistry and Biochemistry, University of Oklahoma, 620 Parrington
Oval, Norman, Oklahoma 73019, Department of Chemistry and Biochemistry, University of Notre Dame,
Notre Dame, Indiana 46556, and Department of Physics, Knox College, Galesburg, Illinois 61401*

Received January 31, 2001

Abstract: The six-coordinate nitrosyl σ-bonded aryl(iron) and -(ruthenium) porphyrin complexes (OEP)Fe-
(NO)(*p*-C$_6$H$_4$F) and (OEP)Ru(NO)(*p*-C$_6$H$_4$F) (OEP = octaethylporphyrinato dianion) have been synthesized
and characterized. Single-crystal X-ray structure determinations reveal an unprecedented bending and tilting
of the MNO group for both {MNO}^{6} species as well as significant lengthening of trans axial bond distances.
In (OEP)Fe(NO)(*p*-C$_6$H$_4$F) the Fe−N−O angle is 157.4(2)°, the nitrosyl nitrogen atom is tilted off of the
normal to the heme plane by 9.2°, Fe−N(NO) = 1.728(2) Å, and Fe−C(aryl) = 2.040(3) Å. In (OEP)Ru-
(NO)(*p*-C$_6$H$_4$F) the Ru−N−O angle is 154.9(3)°, the nitrosyl nitrogen atom is tilted off of the heme normal
by 10.8°, Ru−N(NO) = 1.807(3) Å, and Ru−C(aryl) = 2.111(3) Å. We show that these structural features
are intrinsic to the molecules and are imposed by the strongly σ-donating aryl ligand trans to the nitrosyl.
Density functional-based calculations reproduce the structural distortions observed in the parent (OEP)Fe-
(NO)(*p*-C$_6$H$_4$F) and, combined with the results of extended Hückel calculations, show that the observed bending
and tilting of the FeNO group indeed represent a low-energy conformation. We have identified specific orbital
interactions that favor the unexpected bending and tilting of the FeNO group. The aryl ligand also affects the
Fe−NO π-bonding as measured by infrared and ^{57}Fe Mössbauer spectroscopies. The solid-state nitrosyl stretching
frequencies for the iron complex (1791 cm^{-1}) and the ruthenium complex (1773 cm^{-1}) are significantly reduced
compared to their respective {MNO}^{6} counterparts. The Mössbauer data for (OEP)Fe(NO)(*p*-C$_6$H$_4$F) yield
the quadrupole splitting parameter +0.57 mm/s and the isomer shift 0.14 mm/s at 4.2 K. The results of our
study show, for the first time, that bent Fe−N−O linkages are possible in formally ferric nitrosyl porphyrins.

Introduction

The nature of binding of nitric oxide (NO) to the metal center
in iron porphyrins has received renewed interest since the
discovery that the enzyme that produces NO in the body (NO
synthase) and the enzymatic receptor for NO (soluble guanylyl
cyclase) both contain heme. Bonding descriptions of the metal
nitrosyl linkage (i.e., metal−N−O) generally rely on two types
of formalism.[1] The oxidation-state formalism assigns the linear
NO group as NO$^+$ (isoelectronic with CO) and the bent NO
group as NO$^-$. However, this formalism does not take into
account the *degree* of bending of the MNO fragment and is
often fraught with unrealistic oxidation state assignments. For
example, the tetranitrosyl Cr(NO)$_4$ has four linear NO groups;[2]
hence, the Cr atom should be assigned a 4− charge based on
this formalism. A much more reliable description for MNO
geometry is based on the now widely accepted Enemark−
Feltham notation. In this notation, a nitrosyl complex is
described as a {M(NO)$_x$}^{n} complex, where *x* is the number of
NO ligands, and *n* is the total number of electrons in the metal
d and NO π* orbitals.[3] Importantly, NO is assumed to be a
neutral ligand, and the MNO fragment is considered as a single

unit (i.e., the NO ligand is not assigned a charge, whereas all
of the other ligands are). Thus, for example, the (por)Fe(NO)
and anionic [(por)Fe(NO)X]$^-$ compounds[4] (X = monoanionic
ligand) are classified as {FeNO}^{7} species, whereas the [(por)-
Fe(NO)]$^+$ and the neutral (por)Fe(NO)X compounds are clas-
sified as {FeNO}^{6} species.

To date, two types of Fe−N−O linkages in iron nitrosyl
porphyrins have been characterized by single-crystal X-ray
crystallography.[5,6] The first involves the *linear* Fe−N−O linkage
that is typical of {FeNO}^{6} porphyrin species, trivially known
as the ferric nitrosyl form. The second is the *bent* Fe−N−O
linkage that is typical of {FeNO}^{7} porphyrin complexes and

(3) (a) Feltham, R. D.; Enemark, J. H. *Top. Stereochem.* **1981**, *12*, 155−
215. (b) Enemark, J. H.; Feltham, R. D. *Coord. Chem. Rev.* **1974**, *13*, 339−
406.

(4) Abbreviations: por, a generalized porphyrinato dianion; porph,
unsubstituted porphinato dianion; OEP, dianion of 2,3,7,8,12,13,17,18-
octaethylporphyrin; TPP = dianion of 5,10,15,20-tetraphenylporphyrin; TTP,
dianion of 5,10,15,20-tetra -*p*-tolylporphyrin; TpivPP, dianion of 5,10,15,-
20-α,α,α,α-tetrakis-*o*-pivalamidophenylporphyrin; T(*p*-OCH$_3$)PP, dianion
of 5,10,15,20-tetra-*p*-methoxyphenylporphyrin; Iz, indazole; Pz, pyrazole;
Py, pyridine; Prz, pyrazine; 1-MeIm, 1-methylimidazole; 4-MePip, 4-me-
thylpiperidine; Neop, neopentyl; Mb, myoglobin; N$_p$, porphinato nitrogen
atom.

(5) Cheng, L.; Richter-Addo, G. B. Binding and Activation of Nitric
Oxide by Metalloporphyrins and Heme. In *The Porphyrin Handbook*;
Kadish, K. M., Smith, K. M., Guilard, R., Eds.; Academic Press: New
York, 2000; Vol. 4 (Biochemistry and Binding: Activation of Small
Molecules), pp 219−291.

(6) See Table 6 in ref 5 for a listing of structurally characterized
nitrosylmetalloporphyrins.

† University of Oklahoma.
‡ University of Notre Dame.
§ Knox College.
(1) Richter-Addo, G. B.; Legzdins, P. *Metal Nitrosyls*; Oxford University
Press: New York, 1992.
(2) Hedberg, L.; Hedberg, K.; Satija, S. K.; Swanson, B. I. *Inorg. Chem.*
1985, *24*, 2766−2771.

commonly referred to as the ferrous nitrosyl form. In both types of species a limited variability of the Fe−N−O angle has been observed; the angle in {FeNO}⁶ species ranges from 170° to exactly linear and from 140 to 150° in {FeNO}⁷ species.

Prior to our current study, all iron nitrosyl porphyrins fit into either of these two limiting linear {FeNO}⁶ or bent {FeNO}⁷ categories. We now report a very unusual observation: that the formally {FeNO}⁶ ferric complex (OEP)Fe(NO)(p-C₆H₄F) displays an unexpectedly strongly *bent* and *tilted* Fe−N−O geometry. The synthesis and characterization of the analogous ruthenium species, (OEP)Ru(NO)(p-C₆H₄F), confirms these unexpected structural results. We show that the bending of the MNO group in these rather unusual molecules is due to intrinsic electronic factors.

We have substantiated our experimental findings with hybrid Hartree−Fock density functional and extended Hückel calculations. Other semiempirical MO, ab initio MO, and density functional calculations have been performed to investigate ligand tilting[7] or MNO bending[8−14] in transition metal complexes. Coppens and co-workers have recently reported density functional calculations that approximately reproduce the experimentally observed axial N-atom tilt and Fe−N$_p$ asymmetry in the X-ray structure of the five-coordinate complex, (OEP)Fe(NO).[15] Most recently, Ghosh and Wondimagegn have reported density functional calculations that investigate the specific orbital interactions implicated in nitrosyl ligand tilting in the five-coordinate (por)M(NO) compounds of Fe and Co.[16] Similar findings were subsequently reported by Patchkovskii and Ziegler.[17] In related work, a seminal density functional study of carbon monoxyhemes by Ghosh and Bocian[18] showed an electronic preference for a linear L−Fe−C−O unit but indicated very soft force constants for combined tilting and bending motions of the axial ligands. In contrast, our HF/DF calculations clearly show that the structure of (porph)Fe(NO)(p-C₆H₄F) with *both axial ligands tilted off-axis and with the FeNO group bent represents a minimum-energy structure* whose general features are consistent with the high-quality X-ray diffraction structure. Extended Hückel molecular orbital calculations show the orbital mixing that leads to a low barrier for FeNO bending once the ligands are tilted off the perpendicular.

Experimental Section

All reactions were performed under an atmosphere of argon or prepurified nitrogen using standard Schlenk techniques or in an Innovative Technology Labmaster 100 Dry Box unless stated otherwise. Solvents were distilled from appropriate drying agents under nitrogen just prior to use: CH₂Cl₂ (CaH₂), benzene (Na), hexane (CaH₂ or Na), toluene (Na), and THF (CaH₂).

Chemicals. Octaethylporphyrin, OEPH₂, was purchased from Mid-century Chemicals. (OEP)FeCl was synthesized by a modified literature method.[19,20] (OEP)Ru(CO), NOBF₄, and (p-C₆H₄F)MgBr (1 M in THF or 2 M in ether) were purchased from Aldrich Chemical Co. NO gas was purified by passing it through 4 Å molecular sieves immersed in a dry ice/ethanol slush bath to remove higher oxides of nitrogen.[21] Chloroform-d (99.8%) was obtained from Cambridge Isotope Laboratories and subjected to three freeze−pump−thaw cycles and stored over Linde 4 Å molecular sieves. Elemental analyses were performed by Atlantic Microlab, Norcross, Georgia.

Instrumentation. Infrared spectra were recorded on a BioRad FT-155 FTIR or Perkin-Elmer 883 spectrometer. ¹H NMR spectra were obtained on a Varian XL-400 MHz spectrometer and the signals referenced to the residual signal of the solvent employed. All coupling constants are in Hz. UV−vis spectra were recorded on a Hewlett-Packard HP8453 Diode Array instrument. The solid-state Mössbauer sample was immobilized in Apiezon grease, and the Mössbauer measurements were performed on a constant acceleration spectrometer from 4.2 to 293 K with optional zero field and in a 4-T superconducting magnet system (Knox College).

Preparation of (OEP)Fe(NO)(p-C₆H₄F). The organometallic (OEP)-Fe(p-C₆H₄F) was generated from the reaction of (OEP)FeCl and (p-C₆H₄F)MgBr, according to literature methods.[22,23] The toluene solution containing (OEP)Fe(p-C₆H₄F) was dried with MgSO₄ and loaded on a basic alumina column. The volume of the collected fraction was reduced in vacuo. X-ray quality crystals of (OEP)Fe(NO)(p-C₆H₄F) (v_{NO}, 1791 cm⁻¹ (Nujol)) were obtained by transferring ∼1 mL of the concentrated toluene solution of (OEP)Fe(p-C₆H₄F) to an 8 × 150 mm glass tube inside an extra-long Schlenk tube. NO gas was then bubbled slowly into the solution for less than 1 min, and NO-saturated hexanes were then layered over the solution in the tube. A bulk sample of (OEP)-Fe(NO)(p-C₆H₄F) for Mössbauer measurements was obtained by bubbling NO gas into the concentrated solution of (OEP)Fe(p-C₆H₄F) in a Schlenk tube and layering the solution with NO-saturated hexanes. All manipulations including crystallizations were done in the dark.

Preparation of (OEP)Ru(NO)(p-C₆H₄F). Method I. To a CH₂Cl₂ (20 mL) solution of (OEP)Ru(CO) (0.100 g, 0.151 mmol) was added ClNO (ca. 0.155 mmol in CH₂Cl₂ solution). The mixture was left to stir for 20 min. The color of the solution changed from pink-red to brown-red. The mixture was taken to dryness, and the residue was suspended in THF (40 mL). Excess (p-C₆H₄F)MgBr (0.95 mL, 1.0 M in THF, 0.95 mmol) was added, the IR spectrum indicated the completion of the reaction after 20 min (the 1831 cm⁻¹ band due to the intermediate (OEP)Ru(NO)Cl complex was replaced by a new band at 1761 cm⁻¹), and the color of the near homogeneous solution turned from brown-red to bright red. All of the solvent was removed in vacuo, and the residue was redissolved in CH₂Cl₂ and filtered through silica gel. The solvent was allowed to evaporate under inert atmosphere to generate a purple crystalline solid (OEP)Ru(NO)(p-C₆H₄F)·0.13CH₂-Cl₂ (0.091 g, 0.118 mmol, 78% yield).

Method II. To a CH₂Cl₂ (20 mL) solution of (OEP)Ru(CO) (50 mg, 0.076 mmol) was added NOBF₄ (9 mg, 0.077 mmol). The mixture was left to stir for 30 min, during which time the 1921 cm⁻¹ band in the IR spectrum was replaced by a new band at 1873 cm⁻¹. The color of the solution changed from pink-red to brown-red. All of the solvent was removed in vacuo, and THF (20 mL) was added. Excess (p-C₆H₄F)-MgBr (0.4 mL, 1.0 M in THF, 0.4 mmol) was added, and the reaction was monitored by IR spectroscopy. The reaction reached completion after 10 min (the initial band at 1872 cm⁻¹ was replaced by a band at

(7) Kubacek, P.; Hoffmann, R. *J. Am. Chem. Soc.* **1981**, *103*, 4320−4332.

(8) Rovira, C.; Kunc, K.; Hutter, J.; Ballone, P.; Parrinello, M. *J. Phys. Chem. A* **1997**, *101*, 8914−8925.

(9) Hoffmann, R.; Chen, M. M.-L.; Thorn, D. L. *Inorg. Chem.* **1977**, *16*, 503−511.

(10) Doetschman, D. C. *Chem. Phys.* **1980**, *48*, 307−314.

(11) Loew, G. H.; Kirchner, R. F. *Int. J. Quantum Chem., Quantum Biol. Symp.* **1978**, *5*, 403−415.

(12) Waleh, A.; Ho, N.; Chantranupong, L.; Loew, G. H. *J. Am. Chem. Soc.* **1989**, *111*, 2767−2772.

(13) Halton, M. P. *Inorg. Chim. Acta* **1974**, *8*, 137−142.

(14) Rovira, C.; Kunc, K.; Hutter, J.; Ballone, P.; Parrinello, M. *Int. J. Quantum Chem.* **1998**, *69*, 31−35.

(15) Cheng, L.; Novozhilova, I.; Kim, C.; Kovalevsky, A.; Bagley, K. A.; Coppens, P.; Richter-Addo, G. B. *J. Am. Chem. Soc.* **2000**, *122*, 7142−7143.

(16) Ghosh, A.; Wondimagegn, T. *J. Am. Chem. Soc.* **2000**, *122*, 8101−8102.

(17) Patchkovskii, S.; Ziegler, T. *Inorg. Chem.* **2000**, *39*, 5354−5364.

(18) Ghosh, A.; Bocian, D. F. *J. Phys. Chem.* **1996**, *100*, 6363−6367.

(19) Adler, A. D.; Longo, F. R.; Kampas, F.; Kim, J. *J. Inorg. Nucl. Chem.* **1970**, *32*, 2443−2445.

(20) Buchler, J. W. In *Porphyrins and Metalloporphyrins*; Smith, K. M., Ed.; Elsevier Scientific Publishing: Amsterdam, The Netherlands, 1975; Chapter 5.

(21) Dodd, R. E.; Robinson, P. L. *Experimental Inorganic Chemistry*; Elsevier: Amsterdam, 1954.

(22) Cocolios, P.; Lagrange, G.; Guilard, R. *J. Organomet. Chem.* **1983**, *253*, 65−79.

(23) Guilard, R.; Boisselier-Cocolios, B.; Tabard, A.; Cocolios, P.; Simonet, B.; Kadish, K. M. *Inorg. Chem.* **1985**, *24*, 2509−2520.

Table 1. Crystal Data and Structure Refinement

	(OEP)Ru(NO)(p-C$_6$H$_4$F)	(OEP)Ru(NO)(p-C$_6$H$_4$F)	(OEP)Fe(NO)(p-C$_6$H$_4$F)
formula (fw)	C$_{42}$H$_{48}$FN$_5$ORu (758.92)	C$_{42}$H$_{48}$FN$_5$ORu (758.92)	C$_{42}$H$_{48}$FN$_5$OFe (713.70)
T, K	173(2)	303(2)	130(2)
diffractometer	Siemens P4	Siemens P4	Nonius FAST
crystal system	triclinic	triclinic	triclinic
space group	$P\bar{1}$	$P\bar{1}$	$P\bar{1}$
unit cell dimensions	$a = 10.5223(11)$ Å,	$a = 10.6209(8)$ Å,	$a = 10.487(3)$ Å,
	$\alpha = 96.051(11)°$	$\alpha = 95.705(8)°$	$\alpha = 96.045(15)°$
	$b = 10.8549(14)$ Å,	$b = 10.9386(12)$ Å,	$b = 10.833(3)$ Å,
	$\beta = 97.08(1)°$	$\beta = 97.009(7)°$	$\beta = 97.114(16)°$
	$c = 15.793(2)$ Å,	$c = 15.918(2)$ Å,	$c = 15.804(5)$ Å,
	$\gamma = 99.464(10)°$	$\gamma = 99.610(7)°$	$\gamma = 99.466(16)°$
V, Z	1751.1(4) Å^3, 2	1796.2(3) Å^3, 2	1742.9(9) Å^3, 2
D(calcd), g/cm^3	1.439	1.403	1.360
abs coeff, mm^{-1}	0.495	0.483	0.480
final R indices [$I > 2\sigma(I)$]	R1 = 0.0394, wR2 = 0.0878	R1 = 0.0490, wR2 = 0.0982	R1 = 0.0628, wR2 = 0.1344
R indices (all data)	R1 = 0.0550, wR2 = 0.1158	R1 = 0.0814, wR2 = 0.1313	R1 = 0.0902, wR2 = 0.1496

1761 cm^{-1}). The color of the solution turned from brown-red to bright red, and the product appeared to be more soluble than the intermediate (OEP)Ru(NO)BF$_4$ compound. All of the solvent was removed in vacuo, and the residue was redissolved in CH$_2$Cl$_2$ and filtered through silica gel. The CH$_2$Cl$_2$ solvent was allowed to evaporate under inert atmosphere to generate the purple crystalline product in 82% yield.

Anal. Calcd for C$_{42}$H$_{48}$O$_1$N$_5$Ru$_1$F$_1$·0.13CH$_2$Cl$_2$: C, 65.72; H, 6.32; N, 9.10; Cl, 1.20. Found: C, 65.30; H, 6.35; N, 8.81; Cl, 1.20. IR (CH$_2$Cl$_2$, cm^{-1}): ν_{NO} = 1770. IR (THF, cm^{-1}): ν_{NO} = 1761. IR (KBr, cm^{-1}): ν_{NO} = 1759 s; also 2965 m, 2929 w, 2869 w, 1571 w, 1470 m, 1446 m, 1372 m, 1317 w, 1269 s, 1222 m, 1151 s, 1110 w, 1055 m, 1019 s, 991 w, 960 m, 926 w, 839 m, 810 s, 743 s, 723 w, 714 m, 560 w. ^{1}H NMR (CDCl$_3$, δ): 10.18 (s, 4H, *meso*-H of OEP), 5.28 (s, C*H*$_2$-Cl$_2$), 4.17 (t, $J = 9$, 2H, *m*-H of *p*-C$_6$H$_4$F, overlapping with CH$_3$C*H*$_2$ of OEP), 4.10 (m, 16H, CH$_3$C*H*$_2$ of OEP), 1.94 (t, $J = 8$, 24H, C*H*$_3$-CH$_2$ of OEP), −0.46 (d, 1H, $J = 9$, *o*-H of *p*-C$_6$H$_4$F), −0.48 (d, 1H, $J = 9$, *o′*-H of *p*-C$_6$H$_4$F). UV−vis spectrum (λ (ϵ, mM^{-1} cm^{-1}), 4.74 × 10^{-6} M in CH$_2$Cl$_2$): 360 (82), 404 (144), 555 (17) nm.

X-ray Structure Determinations. Complete crystallographic details, atomic coordinates, anisotropic thermal parameters, and fixed hydrogen atom coordinates are included in the Supporting Information. Details of the crystal data and refinement are given in Table 1.

(i) (OEP)Fe(NO)(p-C$_6$H$_4$F). The structure determination was carried out on a Nonius FAST area-detector diffractometer (at the University of Notre Dame) with a Mo Kα rotating anode source ($\lambda = 0.71073$ Å). Detailed methods and procedures for small-molecule X-ray data collection with the FAST system have been described previously.[24] Data collection was performed at 130(2) K. A dark purple crystal of (OEP)-Fe(NO)(p-C$_6$H$_4$F) was used for the structure determination. The structure was solved using the direct methods program SHELXS-86;[25] subsequent difference Fourier syntheses led to the location of the remaining atoms. The structure was refined against F^2 with the program SHELXL-97, in which all data collected were used including negative intensities. All non-hydrogen atoms were refined anisotropically. Hydrogen atoms were idealized with the standard SHELXL-97 idealization methods.

(ii) (OEP)Ru(NO)(p-C$_6$H$_4$F). The data were collected both at 303(2) K and 173(2) K on a Siemens (Bruker) P4 diffractometer (University of Oklahoma) using Mo Kα radiation ($\lambda = 0.71073$ Å). The data were corrected for Lorentz and polarization effects, and an empirical absorption correction based on ψ scans was applied.[26] The structure was solved by the heavy-atom method using the SHELXTL system,[27] and refined by full-matrix least-squares on F^2 using all reflections. All of the non-hydrogen atoms were refined anisotropically, and the hydrogen atoms were included in the refinement with idealized parameters.

Calculations. All Hartree−Fock density functional (HF/DF) calculations were performed for the lowest-energy singlet state of (porph)-Fe(NO)(p-C$_6$H$_4$F) using the program GAUSSIAN 94.[28,29] The 3-21G basis set was chosen for preliminary calculations because it is deemed the smallest basis set capable of giving reasonable geometries.[30,31] The three-parameter, hybrid HF/DF method used, B3LYP, is widely used and is described in the literature.[29,32] The geometry was fully optimized in C_1 symmetry by using internal coordinates. Since the basis set used for the initial calculations have well-known limitations,[28,30,31,33] we are currently repeating and extending our calculations using larger basis sets.

Qualitative molecular orbital arguments in this paper are based on extended Hückel calculations.[34−37] The basis set included single Slater-type functions for all orbitals except metal 3d orbitals, which were approximated by double-ζ functions. Parameters for the various atoms were obtained from previous calculations reported in the literature[38−40] and are listed in Table S17 (Supporting Information). The geometry for (porph)Fe(NO)(p-C$_6$H$_4$F) was taken from the crystal structure of (OEP)Fe(NO)(p-C$_6$H$_4$F) reported here, the ethyl substituents were replaced by hydrogen atoms, and then the molecule was symmetrized to the C_{2v} point group. Symmetrization was accomplished by using average bond distances and angles from the X-ray structure and giving the porphyrin ring a planar, D_{4h} symmetry structure. All angular distortions preserved the original bond lengths. Qualitative conclusions were confirmed by repeating our extended Hückel calculations using the exact X-ray diffraction core structure of (OEP)Fe(NO)(p-C$_6$H$_4$F).

Results

Syntheses of Complexes. (OEP)Fe(NO)(p-C$_6$H$_4$F) was prepared by the sequential reaction of (OEP)FeCl with (p-C$_6$H$_4$F)-

(24) Scheidt, W. R.; Turowska-Tyrk, I. *Inorg. Chem.* **1994**, *33*, 1314−1318.

(25) Sheldrick, G. M. *Acta Crystallogr.* **1990**, *A46*, 467.

(26) North, A. T. C.; Philips, D. C.; Mathews, F. S. *Acta Crystallogr.* **1968**, *A24*, 351−359.

(27) Siemens *SHELXTL*, Release 5.03 ed.; Siemens, Ed.; Siemens Analytical X-ray Instruments Inc.: Madison, WI, 1994.

(28) Foresman, J. B.; Frisch, A. *Exploring Chemistry with Electronic Structure Methods,* 2nd ed.; Gaussian, Inc.: Pittsburgh, 1995−1996.

(29) Frisch, M. J.; Trucks, G. W.; Schlegel, H. B.; Gill, P. M. W.; Johnson, G. B.; Robb, M. A.; Cheeseman, J. R.; Keith, T. A.; Petersson, G. A.; Montgomery, J. A.; Raghavachari, K.; Al-Laham, M. A.; Zakrzewski, V. G.; Ortiz, J. V.; Foresman, J. B.; Peng, C. Y.; Ayala, P. A.; Wong, M. W.; Andres, J. L.; Replogle, E. S.; Gomperts, R.; Martin, R. L.; Fox, D. J.; Binkley, J. S.; Defrees, D. J.; Baker, J.; Stewart, J. P.; Head-Gordon, M.; Gonzalez, C.; Pople, J. A. *Gaussian 94*; Gaussian, Inc.: Pittsburg, PA, 1995.

(30) Davidson, E. R.; Feller, D. *Chem. Rev.* **1986**, *86*, 681−696.

(31) Hehre, W. J.; Radom, L.; Schleyer, P. V. R.; Pople, J. A. *Ab Initio Molecular Orbital Theory*; Wiley: New York, 1986.

(32) Stephens, P. J.; Devin, F. J.; Chabalowski, C. F.; Frisch, M. J. *J. Phys. Chem.* **1994**, *98*, 11623−11627.

(33) Ziegler, T. *Can. J. Chem.* **1995**, *73*, 743−761 and references therein.

(34) Ammeter, A. B.; Burgi, H.-B.; Thibeault, J. C.; Hoffmann, R. *J. Am. Chem. Soc.* **1978**, *100*, 3686−3692.

(35) Hoffmann, R.; Lipscomb, W. N. *J. Chem. Phys.* **1962**, *36*, 2179−2195.

(36) Jordan, T.; Smith, H. W.; Lohr, L. L., Jr.; Lipscomb, W. N. *J. Am. Chem. Soc.* **1963**, *85*, 846−851.

(37) Wolfsberg, M.; Helmholtz, L. *J. Chem. Phys.* **1952**, *20*, 837−843.

(38) Anderson, A. B.; Hoffmann, R. *J. Chem. Phys.* **1974**, *60*, 4271.

(39) Hoffmann, R. *J. Chem. Phys.* **1963**, *39*, 1397.

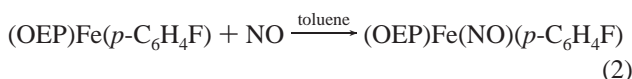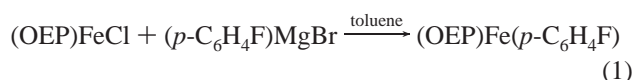(40) Summerville, R. H.; Hoffmann, R. *J. Am. Chem. Soc.* **1978**, *98*, 7240.

Table 2. Representative IR Stretching Frequencies for Nitrosyl Porphyrins of Fe and Ru

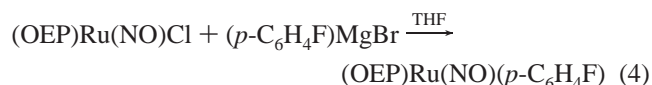| compound	metal coord. no.	${MNO}^n$ $n =$	ν_{NO} $(cm^{-1})^a$	ref
		Iron		
(TPP)Fe(NO)(1-MeIm)	6	7	1625^b	47
(OEP)Fe(NO) triclinic	5	7	1673	48
(OEP)Fe(NO)(CH₃)	6	6	1766	41
(OEP)Fe(NO)(p-C₆H₄Me)	6	6	1785	41
(OEP)Fe(NO)(p-C₆H₄OMe)	6	6	1790	41
(OEP)Fe(NO)(p-C₆H₄F)	6	6	1791	this work
(OEP)Fe(NO)(C₆H₅)	6	6	1795	41
(OEP)Fe(NO)(p-C₆F₄H)	6	6	1839	41
[(OEP)Fe(NO)]⁺	5	6	1862^b	49
(OEP)Fe(NO)(NO₂)	6	6	1883	50
[(OEP)Fe(NO)(Iz)]⁺	6	6	1914	51
		Ruthenium		
(TTP)Ru(NO)(CH₃)	6	6	1743^b	42
(OEP)Ru(NO)(p-C₆H₄F)	6	6	1759^b	this work
(TTP)Ru(NO)(p-C₆H₄F)	6	6	1773^b	42
(OEP)Ru(NO)(OMe)	6	6	1780	52
(OEP)Ru(NO)(SC(Me)₂CH₂−NHC(O)Me)	6	6	1789^b	53
(OEP)Ru(NO)(SC₆F₄H)	6	6	1798^b	54
(OEP)Ru(NO)(OH)	6	6	1806^b	43
(OEP)Ru(NO)Cl	6	6	1827^b	55
(OEP)Ru(NO)(ONO)	6	6	1835^b	43
[(OEP)Ru(NO)(H₂O)]⁺	6	6	1853^b	44
[(OEP)Ru(NO)(O=C(Me)NHCH₂−C(Me)₂SH)]⁺	6	6	1856^b	53

^{a} Nujol mull. *^{b}* KBr pellet.

MgBr (eq 1) and then NO gas (eq 2).

$$(OEP)FeCl + (p\text{-}C_6H_4F)MgBr \xrightarrow{\text{toluene}} (OEP)Fe(p\text{-}C_6H_4F) \tag{1}$$

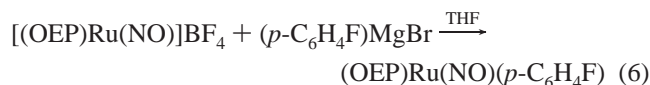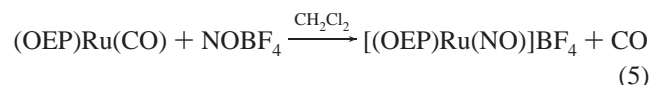$$(OEP)Fe(p\text{-}C_6H_4F) + NO \xrightarrow{\text{toluene}} (OEP)Fe(NO)(p\text{-}C_6H_4F) \tag{2}$$

Because of the air- and light-sensitive nature of (OEP)Fe(NO)-(p-C₆H₄F), we obtained X-ray quality crystals directly from the reaction solution in the dark. This {FeNO}⁶ species, (OEP)Fe-(NO)(p-C₆H₄F), was characterized by IR and Mössbauer spectroscopies. The ν_{NO} of 1791 cm⁻¹ (Nujol) is within the 1766−1839 cm⁻¹ (Nujol) range observed for related (OEP)Fe(NO)R complexes reported by Guilard and Kadish (Table 2).[41]

Two methods were used to prepare the new (OEP)Ru(NO)-(p-C₆H₄F) complex needed for this study. The first is based on the synthesis of the related species, (TTP)Ru(NO)(p-C₆H₄F),[42] and involves the reaction of the previously reported (OEP)Ru-(NO)Cl[43] with the (p-C₆H₄F)MgBr Grignard reagent. We have found that the precursor (OEP)Ru(NO)Cl can be conveniently prepared by nitrosyl chloride addition to (OEP)Ru(CO) (eq 3), and the crude product is sufficiently pure for the next step without any significant loss in yield of the final organometallic product.
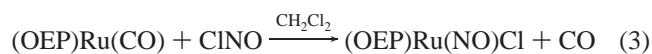
$$(OEP)Ru(CO) + ClNO \xrightarrow{\text{CH}_2\text{Cl}_2} (OEP)Ru(NO)Cl + CO \tag{3}$$

$$(OEP)Ru(NO)Cl + (p\text{-}C_6H_4F)MgBr \xrightarrow{\text{THF}}$$
$$(OEP)Ru(NO)(p\text{-}C_6H_4F) \tag{4}$$

Thus, the subsequent addition (eq 4) of excess (p-C₆H₄F)MgBr to (OEP)Ru(NO)Cl in THF at room-temperature results in the replacement of the starting ν_{NO} band at 1831 cm⁻¹ with a new band at 1761 cm⁻¹ attributed to ν_{NO} of the (OEP)Ru(NO)(p-C₆H₄F) product over a 20 min period. This product is isolated, after workup, analytically pure in 78% yield.

The second method involves the sequential reaction of (OEP)-Ru(CO) with NOBF₄ (in CH₂Cl₂ solvent, eq 5) to produce the intermediate [(OEP)Ru(NO)]BF₄,[44] followed by reaction of this intermediate with (p-C₆H₄F)MgBr (in THF solvent, eq 6).[45]

$$(OEP)Ru(CO) + NOBF_4 \xrightarrow{\text{CH}_2\text{Cl}_2} [(OEP)Ru(NO)]BF_4 + CO \tag{5}$$

$$[(OEP)Ru(NO)]BF_4 + (p\text{-}C_6H_4F)MgBr \xrightarrow{\text{THF}}$$
$$(OEP)Ru(NO)(p\text{-}C_6H_4F) \tag{6}$$

The product of eq 6 was isolated analytically pure in 82% yield after workup. The IR and ¹H NMR spectroscopic properties of (OEP)Ru(NO)(p-C₆H₄F) are consistent with this formulation.

Molecular Structures. The molecular structure of (OEP)-Fe(NO)(p-C₆H₄F) was determined at 130(2) K and is shown in Figure 1a. The relative orientation of the axial ligands is shown in Figure 1b, and the displacements of the porphyrin core atoms from the 24-atom porphyrin plane are shown in Figure 1c. Single-crystal X-ray diffraction data for the (OEP)Ru(NO)(p-C₆H₄F) analogue were collected at low temperatures (173 and 243 K) and at 303 K. No significant differences in the structure were observed at these three temperatures, and the axial C−Ru−NO geometries were virtually identical. The results from the 173 K determination are cited here. The molecular structure of (OEP)Ru(NO)(p-C₆H₄F) is shown in Figure 2a. The relative orientation of the axial ligands is shown in Figure 2b, and the displacements of the porphyrin core atoms from the 24-atom porphyrin plane are shown in Figure 2c. Selected bond lengths and angles for both structures are collected in Table 3.

Discussion

Molecular Structures. There are a number of very interesting structural features for the metal−NO linkages in the iron and ruthenium organometallic porphyrinates described in this paper. These structural features appear to be intrinsic to the complexes and due to the presence of a strongly σ-bonded aryl group. Important structural features include the unexpectedly strong bending of the M−N−O group, the off-axis tilt of the nitrosyl nitrogen atom, and the long M−N(NO) bond distance.

The unexpectedly strong bending of the Fe−N−O group in (OEP)Fe(NO)(p-C₆H₄F) complex is clearly visible in Figure 1a. This is the first time that such a strongly *bent* FeNO geometry in a formally ferric {FeNO}⁶ complex has been observed.[56] The nonbonded interactions described subsequently make evident that crystal packing effects are not responsible for the observed

(41) Guilard, R.; Lagrange, G.; Tabard, A.; Lançon, D.; Kadish, K. M. *Inorg. Chem.* **1985**, *24*, 3649−3656.

(42) Hodge, S. J.; Wang, L.-S.; Khan, M. A.; Young, V. G., Jr.; Richter-Addo, G. B. *Chem. Commun.* **1996**, 2283−2284.

(43) Miranda, K. M.; Bu, X.; Lorkovic, I.; Ford, P. C. *Inorg. Chem.* **1997**, *36*, 4838−4848.

(44) Chen, L.; Yi, G.-B.; Wang, L.-S.; Dharmawardana, U. R.; Dart, A. C.; Khan, M. A.; Richter-Addo, G. B. *Inorg. Chem.* **1998**, *37*, 4677−4688.
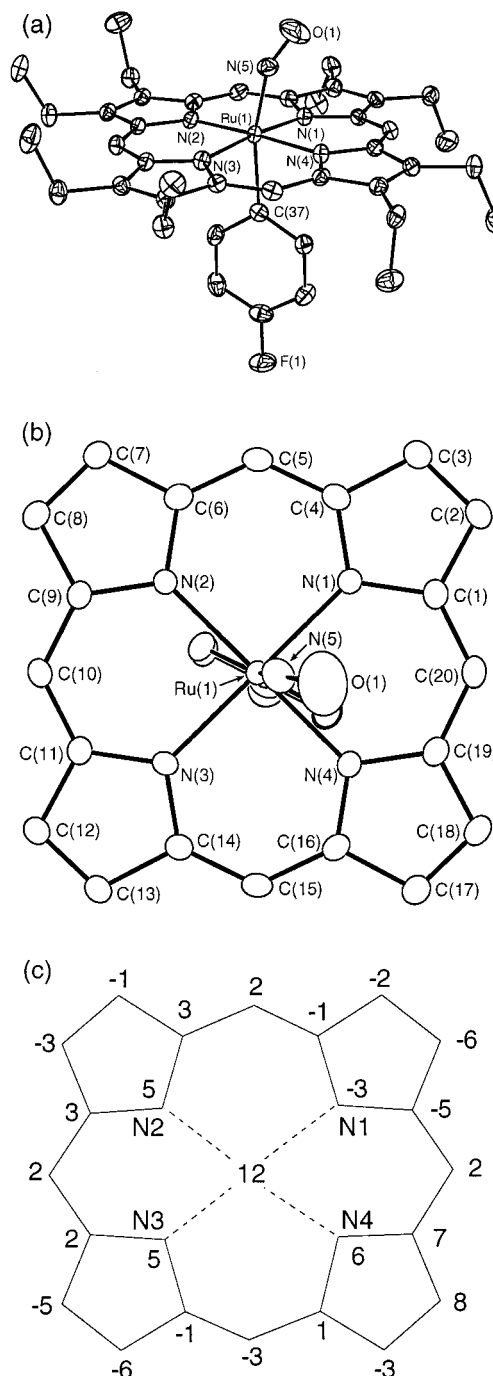
(45) This method has been used to prepare related organometallic osmium nitrosyl porphyrins (ref 46).

(46) Cheng, L.; Chen, L.; Chung, H.-S.; Khan, M. A.; Richter-Addo, G. B.; Young, V. G., Jr. *Organometallics* **1998**, *17*, 3853−3864.

(47) Scheidt, W. R.; Piciulo, P. L. *J. Am. Chem. Soc.* **1976**, *98*, 1913−1919.

(48) Ellison, M. K.; Scheidt, W. R. *J. Am. Chem. Soc.* **1997**, *119*, 7404−7405.

(49) Scheidt, W. R.; Lee, Y. J.; Hatano, K. *J. Am. Chem. Soc.* **1984**, *106*, 3191−3198.
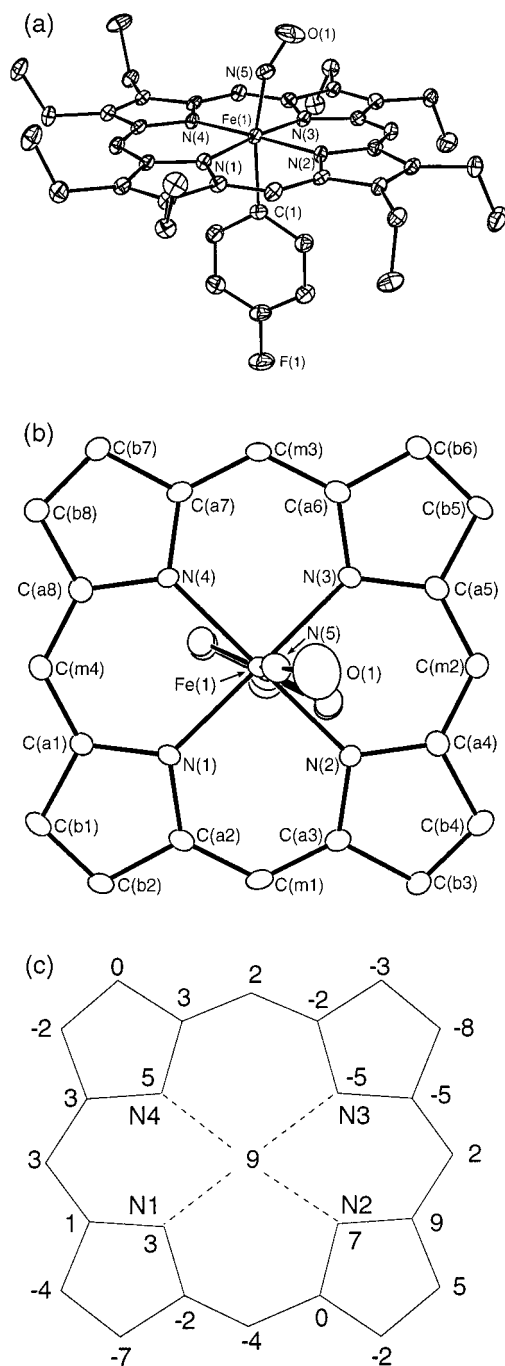
Figure 1. (a) Molecular structure of (OEP)Fe(NO)(p-C$_6$H$_4$F). Hydrogen atoms have been omitted for clarity. (b) Top view (perpendicular to the porphyrin plane) showing the orientation of the axial groups with respect to the porphyrin skeleton. (c) Perpendicular atom displacements from the 24-atom porphyrin plane (in 0.01 Å units).

bending. The Fe−N−O angle in {FeNO}^{6} and {FeNO}^{7} porphyrin species are clustered at near linearity and bent ($\angle\sim145°$), respectively. Thus the value of 157.4(2)° in (OEP)-

(50) Ellison, M. K.; Schulz, C. E.; Scheidt, W. R. *Inorg. Chem.* **1999**, *38*, 100−108.

(51) Ellison, M. K.; Scheidt, W. R. *J. Am. Chem. Soc.* **1999**, *121*, 5210−5219.

(52) Antipas, A.; Buchler, J. W.; Gouterman, M.; Smith, P. D. *J. Am. Chem. Soc.* **1978**, *100*, 3015−3024.

(53) Yi, G.-B.; Khan, M. A.; Powell, D. R.; Richter-Addo, G. B. *Inorg. Chem.* **1998**, *37*, 208−214.

(54) Yi, G.-B.; Khan, M. A.; Richter-Addo, G. B. *Inorg. Chem.* **1996**, *35*, 3453−3454.

(55) Lorkovic, I. M.; Miranda, K. M.; Lee, B.; Bernhard, S.; Schoonover, J. R.; Ford, P. C. *J. Am. Chem. Soc.* **1998**, *120*, 11674−11683.

Figure 2. (a) Molecular structure of (OEP)Ru(NO)(p-C$_6$H$_4$F). Hydrogen atoms have been omitted for clarity. (b) Top view (perpendicular to the porphyrin plane) showing the orientation of the axial groups with respect to the porphyrin skeleton. (c) Perpendicular atom displacements from the 24-atom porphyrin plane (in 0.01 Å units).

Fe(NO)(p-C$_6$H$_4$F) lies *between* the range of angles found in {FeNO}^{6} and {FeNO}^{7} porphyrin species. The Ru−N−O group in (OEP)Ru(NO)(p-C$_6$H$_4$F) and (TTP)Ru(NO)(p-C$_6$H$_4$F) are also significantly bent. At 154.9° and 152° respectively, these Ru−N−O groups are clearly the most bent of the {RuNO}^{6} species listed in Table 4.

(56) Photoreduction of the (por)M(NO)(R) complexes by the X-ray beam is unlikely, since the bent MNO geometry was observed after very short data collection times (for the (OEP)Fe− and (TTP)Ru− complexes, using area detectors) or longer data collection times (for the (OEP)Ru− complex, using a single-point detector). Other {FeNO}^{6} complexes under the same conditions do not get reduced. We do note that a probable photoreduction of the ferric nitrophorin−NO complex to the ferrous derivative has been reported (ref 57).

Table 3. Selected Bond Lengths and Angles for (OEP)M(NO)(p-C$_6$H$_4$F)

Bond Lengths (Å)			
(OEP)Fe(NO)(p-C$_6$H$_4$F)		(OEP)Ru(NO)(p-C$_6$H$_4$F)	
Fe(1)−N(1)	2.001(2)	Ru(1)−N(3)	2.052(3)
Fe(1)−N(2)	2.024(2)	Ru(1)−N(4)	2.059(3)
Fe(1)−N(3)	2.023(2)	Ru(1)−N(1)	2.068(3)
Fe(1)−N(4)	2.015(2)	Ru(1)−N(2)	2.056(3)
Fe(1)−N(5)	1.728(2)	Ru(1)−N(5)	1.807(3)
N(5)−O(1)	1.153(3)	N(5)−O(1)	1.146(4)
Fe(1)−C(1)	2.040(3)	Ru(1)−C(37)	2.111(3)

Bond Angles (deg)			
(OEP)Fe(NO)(p-C$_6$H$_4$F)		(OEP)Ru(NO)(p-C$_6$H$_4$F)	
Fe(1)−N(5)−O(1)	157.4(2)	Ru(1)−N(5)−O(1)	154.9(3)
C(1)−Fe(1)−N(5)	168.85(11)	C(37)−Ru(1)−N(5)	166.59(13)
N(5)−Fe(1)−N(1)	98.56(10)	N(5)−Ru(1)−N(3)	99.07(12)
N(5)−Fe(1)−N(2)	84.43(10)	N(5)−Ru(1)−N(4)	83.47(13)
N(5)−Fe(1)−N(3)	87.09(10)	N(5)−Ru(1)−N(1)	86.67(12)
N(5)−Fe(1)−N(4)	97.24(10)	N(5)−Ru(1)−N(2)	99.74(13)
C(1)−Fe(1)−N(1)	87.83(10)	C(37)−Ru(1)−N(3)	87.92(11)
C(1)−Fe(1)−N(2)	86.43(10)	C(37)−Ru(1)−N(4)	85.09(12)
C(1)−Fe(1)−N(3)	86.51(9)	C(37)−Ru(1)−N(1)	86.35(11)
C(1)−Fe(1)−N(4)	91.89(10)	C(37)−Ru(1)−N(2)	91.70(12)

In addition, the Fe−N(O) vector in (OEP)Fe(NO)(p-C$_6$H$_4$F) is tilted off the normal to the mean porphyrin plane by 9.2° (α in Table 5). Other nitrosyl porphyrin derivatives have also been shown to display off-axis tilting of the nitrosyl nitrogen atom.[42,48,65−67] The NO group is further tilted 22.6° (β) from the Fe−N(O) vector in the direction away from the porphyrin normal. The C(1) atom of the axial phenyl group is also tilted off the normal to the 24-atom porphyrin plane. The tilt of 3.1° (γ) is toward the NO group; the C−Fe−N angle is 168.85 (11)°. Distortions from axial symmetry for (OEP)Ru(NO)(p-C$_6$H$_4$F) are also shown in Table 5. The axial N(5) atom of the NO group is tilted 10.8° (α) from the normal to the 24-atom porphyrin plane (10.2° from the normal to the four-nitrogen plane). The axial C(37) atom of the aryl ligand is tilted by 3.5° (γ) in the general direction of the NO tilt. The angles for these off-axis tilts for the related (TTP)Ru(NO)(p-C$_6$H$_4$F) complex[42] are shown for comparison in Table 5.

The axial bond distances in the formally ferric {FeNO}⁶ complex (OEP)Fe(NO)(p-C$_6$H$_4$F) are also unusual. The Fe−N(O) distance of 1.728(2) Å is very long in comparison to those of other {FeNO}⁶ complexes where the range of Fe−N(O) distances is 1.627(2)−1.671(2) Å. Indeed, the Fe−N(O) distance in (OEP)Fe(NO)(p-C$_6$H$_4$F) is within the range of values observed for the ferrous {FeNO}⁷ porphyrin species given in

Table 4 (1.717(7)−1.740(7) Å). It is thus almost 0.1 Å longer than expected. Similarly, the Ru−N(NO) distance in (OEP)-Ru(NO)(p-C$_6$H$_4$F) is very long at 1.807(3) Å. In comparison with those of other {RuNO}⁶ complexes, where the bond lengths have been determined with sufficient accuracy, the Ru−N(NO) bond length in (OEP)Ru(NO)(p-C$_6$H$_4$F) is on average 0.07 Å longer (Table 4). The observed M−N(NO) lengthening and M−N−O bending in these {MNO}⁶ species results from the addition of a strongly σ-bonding axial ligand trans to the nitrosyl in both the iron and ruthenium derivatives. Furthermore, the axial Fe−C(aryl) bond length of 2.040(3) Å in (OEP)Fe(NO)-(p-C$_6$H$_4$F) is 0.085 Å longer than in the related species, (TPP)-Fe(C$_6$H$_5$) (Table 6). A similar lengthening of the axial Ru−C(aryl) bond by 0.1 Å is observed in (OEP)Ru(NO)(p-C$_6$H$_4$F) versus (OEP)Ru(C$_6$H$_5$) (Table 6). We note that although the axial Ru−C(aryl) bond length of 2.111(3) Å in (OEP)Ru(NO)-(p-C$_6$H$_4$F) is within the 1.943(9) Å (in Ru(o-tol)$_4$)[74] to 2.250-(4) Å (in (dmpe)$_2$RuH(C$_6$F$_5$))[75] range observed for other Ru−C(aryl) bonds in coordination compounds, it is well outside the 1.999(4)−2.005(7) Å range previously observed for (por)Ru−C(aryl) bonds (Table 6). Clearly, the nitrosyl ligand exerts a structural trans effect reflected in the elongated M−C bond distances in both derivatives.

The average Fe−N$_p$ bond length in (OEP)Fe(NO)(p-C$_6$H$_4$F) is 2.016(11) Å, which is almost 0.02 Å longer than the average Fe−N$_p$ bond length for all of the other {FeNO}⁶ derivatives (Table 4). Indeed, the Fe−N$_p$ bond length is slightly longer than that of the most accurately determined five-coordinate {FeNO}⁷ structure. In contrast, the average Ru−N$_p$ bond length of 2.059(7) Å in (OEP)Ru(NO)(p-C$_6$H$_4$F) is not longer than those of other {RuNO}⁶ derivatives (Table 4). However, the average metal−porphyrinato nitrogen distances in both (OEP)Fe(NO)-(p-C$_6$H$_4$F) and (OEP)Ru(NO)(p-C$_6$H$_4$F) are longer (by ca. 0.02 and 0.03 Å respectively) than those found in other six-coordinate, low-spin d⁵ species, although in the ruthenium case there are very few examples with which to compare. The reason for this M−N$_p$ elongation is not clear. However, it could be due to the presence of the strongly σ-donating anionic ligand trans to the nitrosyl.

In both (OEP)Fe(NO)(p-C$_6$H$_4$F) and (OEP)Ru(NO)(p-C$_6$H$_4$F) the metal atom is displaced slightly toward the nitrosyl ligand (by 0.09 Å in Fe and 0.12 Å in Ru). Similar small out-of-plane displacements toward the nitrosyl ligand are seen for all of the six-coordinate {MNO}⁶ species where the accuracy of the X-ray structural results are not limited by axial ligand disorder. The porphyrin plane is unremarkably planar as can be seen from Figures 1c and 2c. Figures 1b and 2b show the orientation of the axial ligands with respect to the porphyrin plane. The dihedral angle between the Fe−N−O plane and the plane defined as N(5)−Fe−N(2) is 38.8°. The similarly defined dihedral angle for the phenyl ligand is 19°. This angle is smaller than the phenyl dihedral angle found in (OEP)Ru(C$_6$H$_5$) and

(57) Ding, X. D.; Weichsel, A.; Andersen, J. F.; Shokhireva, T. K.; Balfour, C.; Pierik, A. J.; Averill, B. A.; Montfort, W. R.; Walker, F. A. *J. Am. Chem. Soc.* **1999**, *121*, 128−138.

(58) Yi, G.-B.; Chen, L.; Khan, M. A.; Richter-Addo, G. B. *Inorg. Chem.* **1997**, *36*, 3876−3885.

(59) Ellison, M. K.; Schulz, C. E.; Scheidt, W. R. *Inorg. Chem.* **2000**, *39*, 5102−5110.

(60) Scheidt, W. R.; Frisse, M. E. *J. Am. Chem. Soc.* **1975**, *97*, 17−21.

(61) Scheidt, W. R.; Brinegar, A. C.; Ferro, E. B.; Kirner, J. F. *J. Am. Chem. Soc.* **1977**, *99*, 7315−7322.

(62) Bohle, D. S.; Hung, C.-H.; Smith, B. D. *Inorg. Chem.* **1998**, *37*, 5798−5806.

(63) Bohle, D. S.; Goodson, P. A.; Smith, B. D. *Polyhedron* **1996**, *15*, 3147.

(64) Bohle, D. S.; Hung, C.-H.; Powell, A. K.; Smith, B. D.; Wocadlo, S. *Inorg. Chem.* **1997**, *36*, 1992−1993.

(65) Scheidt, W. R.; Duval, H. F.; Neal, T. J.; Ellison, M. K. *J. Am. Chem. Soc.* **2000**, *122*, 4651−4659 and references therein.

(66) Scheidt, W. R.; Ellison, M. K. *Acc. Chem. Res.* **1999**, *32*, 350−359.

(67) Ellison, M. K.; Scheidt, W. R. *Inorg. Chem.* **1998**, *37*, 382−383.

(68) Ke, M.; Rettig, S. J.; James, B. R.; Dolphin, D. *J. Chem. Soc., Chem. Commun.* **1987**, 1110−1112.

(69) Alexander, C. S.; Rettig, S. J.; James, B. R. *Organometallics* **1994**, *13*, 2542−2544.

(70) Seyler, J. W.; Fanwick, P. E.; Leidner, C. R. *Inorg. Chem.* **1990**, *29*, 2021−2023.

(71) Galardon, E.; Le Maux, P.; Toupet, L.; Simonneaux, G. *Organometallics* **1998**, *17*, 565−569.

(72) Doppelt, P. *Inorg. Chem.* **1984**, *23*, 4009−4011.

(73) Balch, A. L.; Olmstead, M. M.; Safari, N.; St. Claire, T. N. *Inorg. Chem.* **1994**, *33*, 2815−2822.

(74) Savage, P. D.; Wilkinson, G.; Motevalli, M.; Hursthouse, M. B. *J. Chem. Soc., Dalton Trans.* **1988**, 669−671.
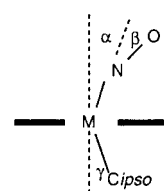
(75) Whittlesey, M. K.; Perutz, R. N.; Moore, M. H. *Chem. Commun.* **1996**, 787−788.

Table 4. Selected Comparisons for Axial Bonding Parameters in {MNO}[6] and {MNO}[7] Metalloporphyrins

complex	M−Np [a]	M−N$_{NO}$ [a]	∠MNO [b]	M−L [a]	N−O [a]	Δ [a,c]	ref
A. {FeNO}[6] Metalloporphyrin Derivatives							
[(OEP)Fe(1-MeIm)(NO)]$^+$	2.003(5)	1.6465(17)	177.28(17)	1.9889(16)	1.135(2)	0.02	51
[(OEP)Fe(Pz)(NO)]$^+$	2.004(5)	1.627(2)	176.9(3)	1.988(2)	1.141(3)	0.01	51
[(OEP)Fe(Iz)(NO)]$^+$	1.996(4)	1.632(3)	177.6(3)	2.010(3)	1.136(4)	0.04	51
{[(OEP)Fe(NO)]$_2$Prz}$^{2+}$	1.995(8)	1.632(3)	176.5(3)	2.039(2)	1.131(4)	0.06	51
[(TPP)Fe(H$_2$O)(NO)]$^+$	1.999(6)	1.652(5)	174.4(10)	2.001(5)	1.150	0.0[d]	49
[(TPP)Fe(HO-i-C$_5$H$_{11}$)(NO)]$^{+e}$	2.013(3)	1.776(5)	177.1(7)	2.063(3)	0.925(6)	0.05[f]	58
(TpivPP)Fe(NO$_2$)(NO)	1.996(4)	1.671(2)	169.3(2)	1.998(2)	1.144(3)	0.09	50
[(OEP)Fe(NO)]ClO$_4$•CHCl$_3$	1.994(1)	1.644(3)	176.9(3)		1.112(4)	0.29	49
[(OEP)Fe(NO)]ClO$_4$	1.994(5)	1.6528(13)	173.19(13)		1.140(2)	0.32	59
(OEP)Fe(NO)(p-C$_6$H$_4$F)	2.016(11)	1.728(2)	157.4(2)	2.040(3)	1.153(3)	0.09	this work
B. {FeNO}[7] Metalloporphyrin Derivatives							
(TPP)Fe(NO)	2.001(3)	1.717(7)	149.2(6)		1.122(12)	0.21	60
(OEP)Fe(NO)	2.010(13)	1.7307(7)	142.74(8)		1.1677(11)	0.27	48
(TPP)Fe(NO)(1-MeIm)	2.008(12)	1.743(4)	142.1(6)	2.180(4)	1.121(8)	0.07	47
(TPP)Fe(NO)(4-MePip)(**1**)	2.004(9)	1.721(10)	138.5(11)	2.328(10)	1.141(13)	0.09	61
(TPP)Fe(NO)(4-MePip)(**2**)	1.998(10)	1.740(7)	143.7(6)	2.463(7)	1.112(9)	0.11	61
C. {RuNO}[6] Metalloporphyrin Derivatives							
(TPP)Ru(NO)(ONO)	2.047(5)	1.72(2)	180.0	1.90(2)	1.12(2)	0.0[d]	43
(OEP)Ru(NO)(ONO)	2.060(5)	1.758(7)	174.0(8)	1.984(6)	1.177(9)	NR[g]	43
(TTP)Ru(NO)(ONO)	2.053(6)	1.752(6)	173.3(6)	1.998(6)	1.152(9)	0.13	62
(TTP)Ru(NO)(OMe)	2.050(3)	1.84(4)[h]	180.0	1.80(5)[h]	NR[g]	0.0[d]	63
(TTP)Ru(NO)(OH)	2.055(5)	1.751(5)	167.4(6)	1.943(5)	1.142(8)	0.05	62
(TPP)Ru(NO)(OH)	2.050(4)	1.726(9)	180.0	1.873(11)	1.179(9)	0.0[d]	43
(OEP)Ru(NO)(OH)	2.060(3)	1.723(11)	173.7(12)	1.956(11)	1.155(14)	NR[g]	43
[(OEP)Ru(NO)(H$_2$O)]$^+$	2.041(4)	1.888(5)[h]	171.0(7)	1.888(5)[h]	1.138(12)	0.0[d]	44
(TTP)Ru(NO)(NSO)	2.055(4)	1.737(5)	170.2(5)	2.022(5)	1.160(6)	NR[g]	64
(OEP)Ru(NO)(SC(Me)$_2$CH$_2$NHC(O)Me)	2.060(2)	1.769(3)	172.8(3)	2.3901(10)	1.114(4)	0.07	53
[(OEP)Ru(NO)(O=C(Me)NHCH$_2$C(Me)$_2$SH)]$^+$	2.050(8)	1.708(6)	177.8(5)	2.049(4)	1.141(7)	0.10	53
(TTP)Ru(NO)(p-C$_6$H$_4$F)	2.05(2)	1.807	152	2.095(6)	1.159	NR[g]	42
(OEP)Ru(NO)(p-C$_6$H$_4$F)	2.059(7)	1.807(3)	154.9(3)	2.111(3)	1.146(4)	0.12	this work

[a] Values given in Å. [b] Values given in degrees. [c] Displacement of metal from 24-atom porphyrin plane toward NO. [d] Metal is exactly in-plane due to symmetry. [e] This complex displayed extensive disorder. [f] Displacement of the metal from the four-nitrogen mean plane. [g] Not reported. [h] The axial ligands are disordered over two positions due to crystallographic symmetry.

Table 5. Axial Ligand Tilts (deg) in Six-Coordinate (Por)M(NO)(Aryl) Compounds[a]

compound	α	β	γ	angle between Ph and MNO planes	reference
(OEP)Fe(NO)(p-C$_6$H$_4$F)[b]	9.2	22.6	3.1	19.8	this work
(OEP)Ru(NO)(p-C$_6$H$_4$F)[c]	10.8	25.1	3.5	16.1	this work
(TTP)Ru(NO)(p-C$_6$H$_4$F)[c]	12.0	27.8	4.3	14.0	42

[a] The α and γ angles are with respect to the normal to the 24-atom mean porphyrin plane. [b] Data collected at 130(2) K. [c] Data collected at 173(2) K.

(TPP)Fe(C$_6$H$_5$) where the phenyl ligands more nearly bisect the N$_p$−M−N$_p$ angle.[68,72] As in the iron case, the axial aryl and RuNO groups are not coplanar, displaying an angle of 16.1° between the six-carbon aryl plane and the RuNO plane (Table 5).

The crystal packing of (OEP)Fe(NO)(p-C$_6$H$_4$F) is shown in Figure 3. The closest intermolecular distance involving the NO group is between two nitrosyl oxygens, with the O(1)•••O(1A) distance of 2.92 Å. The nonbonded distance between two oxygen atoms of (hypothetical) linear NO groups on adjacent molecules was calculated to be 2.88 Å. The next closest intermolecular distance (3.58 Å) is that between the nitrosyl N(5) and an ethyl substituent C(72B) atom on a neighboring molecule (more distances are listed in the caption of Figure 3).

Table 6. Iron and Ruthenium Porphyrin Compounds with Axial Alkyl/Aryl (Non-Carbonyl) Ligands

compound	M−C (Å)	reference
(OEP)Ru(C$_6$H$_5$)	2.005(7)	68
(OEP)Ru(Neop)	2.069(7)	69
	2.12(1)	
[(OEP)Ru(Neop)]$_2$(μ−Li)$_2$	2.100(3)	69
[(OEP-N-Ph)Ru(C$_6$H$_5$)]BF$_4$	1.999(4)	70
(TPP)Ru{=C(CO$_2$Et)$_2$}(MeOH)	1.829(9)	71
(TTP)Ru(NO)(p-C$_6$H$_4$F)	2.095(6)	42
(OEP)Ru(NO)(p-C$_6$H$_4$F)	2.111(3)	this work
(TPP)Fe(C$_6$H$_5$)	1.955(3)	72
(T(p-OCH$_3$)PP)Fe(C(O)(n−Bu))	1.965(12)	73
(T(p-OCH$_3$)PP)Fe(CH$_3$)	1.979(9)	73
(OEP)Fe(NO)(p-C$_6$H$_4$F)	2.040(3)	this work

The crystal packing diagram of the ruthenium complex, (OEP)-Ru(NO)(p-C$_6$H$_4$F), is given in the Supporting Information (Figure S1). The intermolecular contacts are similar to those of the isomorphous Fe analogue: the NO groups of two adjacent molecules also point toward each other, with an O(1)•••O(1A) distance of 2.88 Å; the next closest intermolecular contacts are over 3.56 Å and are listed in the caption of Figure S1. The crystal packing diagram of (TTP)Ru(NO)(p-C$_6$H$_4$F) is also given in the Supporting Information (Figure S2). The packing in the tetraaryl derivative is clearly different from the OEP derivatives. The closest intermolecular distance involving the NO group in this derivative is between the oxygen atom and a nearby tolyl group at an O(1)•••C(18A) distance of 3.23 Å. Other pertinent intermolecular distances are greater than 3.35 Å and are listed in the figure caption. There is thus no evidence that the M−N−O group in any of the three structures is significantly affected by crystal packing.
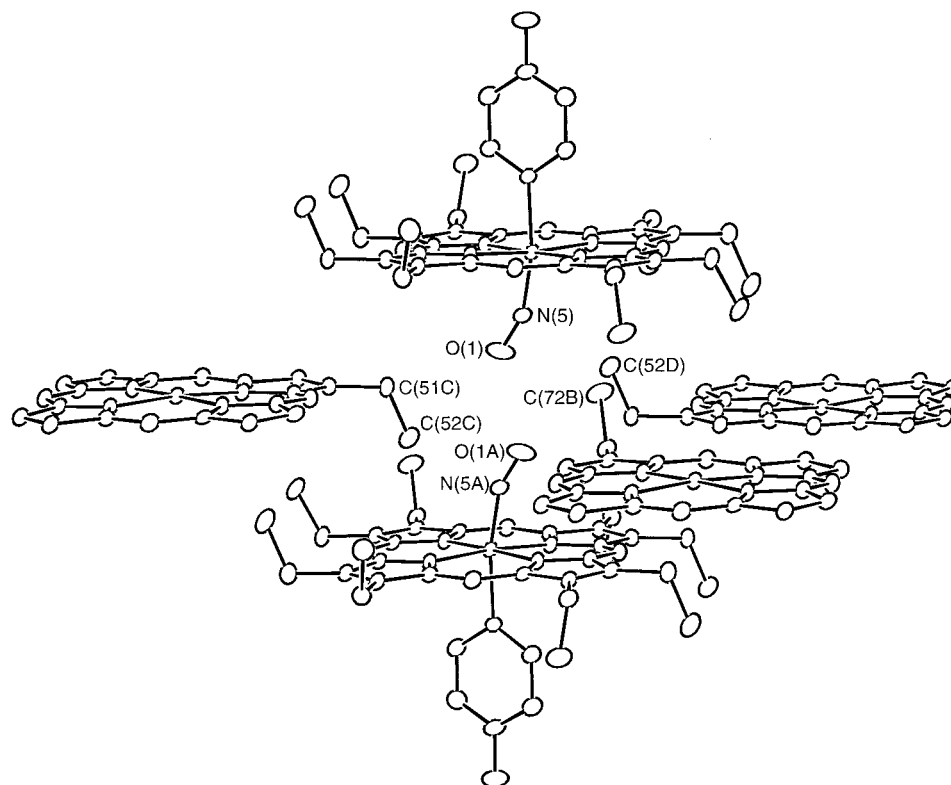
Figure 3. Crystal packing diagram for (OEP)Fe(NO)(p-C$_6$H$_4$F) showing symmetry-related units. The axial NO and aryl groups, as well as most of the ethyl substituents, have been omitted for three of the molecules for the sake of clarity. Closest intermolecular contacts in Å: O(1)⋯O(1A) = 2.92, N(5)⋯C(72B) = 3.58, O(1)⋯C(51C) = 3.62, O(1)⋯C(52C) = 3.64, O(1)⋯C(72B) = 3.68, N(5)⋯C(52D) = 3.78. Symmetry operators used to generate equivalent molecules: A = −x, −y+1, −z+1; B = −x, −y, −z+1; C = −x+1, −y+1, −z+1; D = x−1, y, z.

The unusual geometry of the M−N−O group in these {MNO}⁶ species is also reflected in the observed nitrosyl stretching frequencies which should be quite sensitive to the electronic structure at the metal center. (OEP)Fe(NO)(p-C$_6$H$_4$F) has an unusually low nitrosyl stretching frequency of 1791 cm⁻¹ compared to all of the structurally characterized five- or six-coordinate {FeNO}⁶ porphyrin complexes which have a ν_{NO} range of 1862−1937 cm⁻¹ and which have linear or nearly linear Fe−N−O groups (angles range from 169.3 to 180.0°).[66] Some representative nitrosyl stretching frequencies are listed in Table 2 for iron and ruthenium porphyrin species. The nitrosyl stretching frequencies in five- or six-coordinate {FeNO}⁷ porphyrin complexes are much lower (1616−1690 cm⁻¹). The Fe−N−O groups in these species are bent with angles ranging from 138.1 to 149.2°. The structurally characterized (OEP)Fe-(NO)(p-C$_6$H$_4$F) species has an Fe−N−O angle of 157.4(2)° which is intermediate between the {FeNO}⁶ and {FeNO}⁷ porphyrin complexes. It is also evident from the values given in this table that the σ-bonded alkyl or aryl(iron) derivatives have nitrosyl stretching frequencies intermediate between the {FeNO}⁷ and {FeNO}⁶ derivatives. Although the other σ-bonded alkyl or aryl(iron) derivatives given in the table have not been structurally characterized, it is tempting to suggest a continuum of bent Fe−N−O groups with the most strongly donating methyl derivative having the most bent Fe−N−O group and the least donating tetrafluorophenyl derivative having a near linear Fe−N−O group. Indeed such a suggestion was made earlier,[41] without any structural data. Attempts to structurally characterize these species are in progress. The ruthenium derivatives should show similar trends. (OEP)Ru(NO)(p-C$_6$H$_4$F) has the lowest nitrosyl stretching frequency (for the OEP derivatives) of 1759 cm⁻¹ and the most bent angle of 154.9(3)°. This observation is consistent with the presence of

the strongly σ-interacting trans R group and subsequent increased back-donation of electron density onto the NO ligand. All of the other structurally characterized nonorganometallic {RuNO}⁶ species have linear or near linear Ru−N−O angles. The TTP derivative (TTP)Ru(NO)(CH$_3$), which has not been structurally characterized, has an even lower ν_{NO} as a result of the more strongly donating methyl group trans to the nitrosyl. No ruthenium porphyrin compounds of the {RuNO}⁷ formulation have been reported; hence, a comparison between the {RuNO}⁶ and {RuNO}⁷ systems cannot be made at this time.

Quantum Chemical Studies of (porph)Fe(NO)(p-C$_6$H$_4$F). Extended Hückel molecular orbital (MO)[34−37] and preliminary hybrid Hartree−Fock (HF/DF) density functional calculations[33,76−78] were done to investigate orbital energy changes upon (i) tilting the p-C$_6$H$_4$F and NO ligands off the molecular axis and (ii) bending the NO ligand at the nitrogen.

A complete B3LYP hybrid HF/DF geometry optimization was performed for the (porph)Fe(NO)(p-C$_6$H$_4$F) molecule starting from the experimental, X-ray diffraction geometry. The quantitative accuracy of the HF/DF calculation is limited by the small basis set size, but calculated bond distances for the optimized structure are qualitatively similar to those determined by X-ray diffraction (compared in Figure 4). In the calculated minimum-energy structure, the Fe−N (NO) bond is tilted 11.3° (α) from the perpendicular to the four-nitrogen porphyrin plane, whereas the Fe−C bond is tilted 4.4° (γ). The calculated tilt angles both agree well with the experimentally determined angles, and as in the X-ray structure, both ligands are tilted in the same general direction. In the calculated structure, projections of the Fe−

(76) Ghosh, A. *Acc. Chem. Res.* **1998**, *31*, 189−198.
(77) Parr, R. G.; Yang, W. *Density-Functional Theory of Atoms and Molecules*; Oxford University Press: New York, 1989.
(78) Ziegler, T. *Chem. Rev.* **1991**, *91*, 651−667.
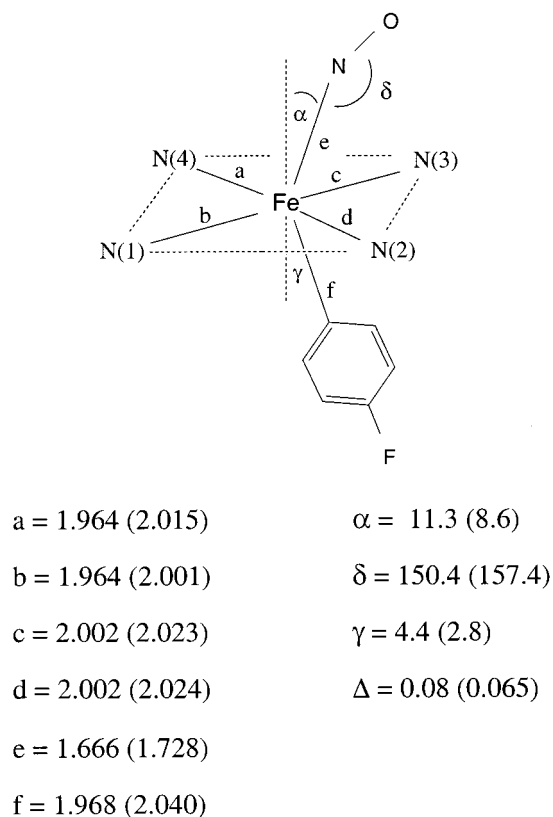
Figure 4. Selected geometrical parameters (in Å and degrees) for (porph)Fe(NO)(p-C_6H_4F), calculated by using the B3LYP hybrid Hartree−Fock/density functional method, compared with corresponding parameters for (OEP)Fe(NO)(p-C_6H_4F), determined by X-ray diffraction (in parentheses). The tilting angles and atom displacement (Δ) are with respect to the four-nitrogen porphyrin plane.

N−O and phenyl planes exactly bisect an N_p−Fe−N_p angle. The calculated structure also shows a significant bending of the FeNO group (150.4°, δ in Figure 4). The iron atom was found to be 0.08 Å out of the four pyrrole nitrogen atom plane, toward the NO ligand (0.06 Å experimental). Although the calculated conformation of the porphyrin ring is slightly ruffled, several different conformations probably have similar energies. The calculated NO distance was 1.193 Å (1.153(3) Å experimental). The calculated Fe−N(NO) distance of 1.666 Å is 0.062 Å shorter than the experimental distance of 1.728(2) Å, and the calculated Fe−C distance (1.968 Å) is 0.072 Å shorter than the experimentally determined Fe−C distance (2.040(3) Å). Calculated Fe−N_p distances show differences of similar magnitudes, but the asymmetry of the Fe−N_4(porph) core is consistent with that determined experimentally for (OEP)Fe-(NO)(p-C_6H_4F). Specifically, the Fe−N_p bonds farthest from the aryl and NO ligands are shorter than the Fe−N_p bonds closer to the axial ligands. The shorter calculated distances are 1.964 Å, compared to experimental distances of 2.001(2) Å and 2.015-(2) Å, whereas the longer calculated distances are 2.002 Å compared with experimental distances of 2.024(2) Å and 2.023(2) Å. We note that this experimentally observed asymmetry in the Fe−N_4(por) core (reproduced by calculations) is opposite to that observed in the five-coordinate (OEP)Fe(NO) compound.[48]

Initial extended Hückel calculations for (porph)Fe(NO)(p-C_6H_4F) were performed for model structures with the C−Fe−N and Fe−N−O angles fixed at 180° (as described in the Experimental Section and Supporting Information Table S17). The frontier molecular orbitals for this structure are described
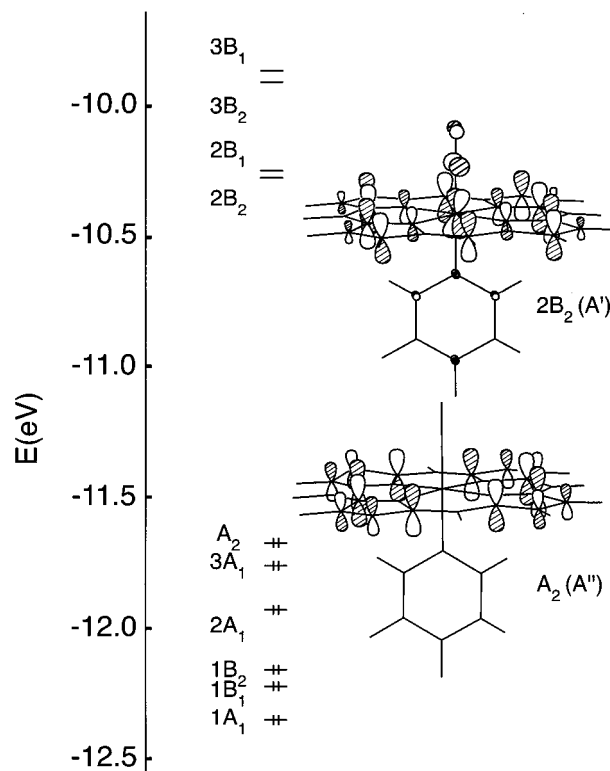

Figure 5. Molecular orbital energy level diagram of (porph)Fe(NO)-(p-C_6H_4F). The B_2 symmetry LUMO and the A_2 symmetry HOMO are also shown.

in detail in the following paragraphs. The ligands were then tilted off the molecular symmetry axis by reducing the C−Fe−N(O) angle, and finally, the Fe−N−O angle was bent. Other exploratory calculations were performed to determine whether FeNO bending could occur independently of ligand tilting off the symmetry axis and to determine whether the orientation of the p-C_6H_4F ligand exerts a substantial electronic effect on the direction of ligand tilting and FeNO bending. Although some of the calculations described below refer to an idealized structure of (porph)Fe(NO)(p-C_6H_4F), qualitative conclusions were confirmed by repeating our calculations using the X-ray diffraction core structure of (OEP)Fe(NO)(p-C_6H_4F) (with the Fe atom placed in the plane of the porphyrin and the ethyl groups replaced with hydrogens).

Figure 5 shows the frontier molecular orbital energy level diagram of (porph)Fe(NO)(p-C_6H_4F), derived from extended Hückel calculations. Orbitals with the correct symmetry to form σ bonds have A_1 symmetry, whereas those with appropriate symmetry to form π bonds have B_1 or B_2 symmetry. The approximately nonbonding orbitals are labeled $1A_1$ and $3A_1$. The porphyrin contribution to the $1A_1$ orbital has the nodal structure of A_{2u} in Gouterman's four-orbital model of porphyrin electronic structure (different symmetry labels arise because of the lower symmetry of the nitrosyl complex and because of our choice of orientation for the x and y axes). The $2A_1$ orbital of (porph)Fe(NO)(p-C_6H_4F) is composed mainly of the metal $d_{x^2-y^2}$ atomic orbital which has the wrong nodal structure to overlap with the NO nitrogen lone pair. The Fe−NO π-bonding molecular orbitals ($1B_1$ and $1B_2$) consist of a mixture of iron d_{xz} or d_{yz} orbitals, respectively, with the NO π^* orbitals to give a strong π-bonding interaction. The molecule's HOMO is the Fe−NO nonbonding orbital labeled A_2, illustrated in Figure 5, and concentrated on the porphyrin ring. A_2 has no contribution from the iron and corresponds to the A_{1u} orbital in the four-orbital model of the porphyrin. The HOMO's composition

$+ \lambda$

$=$

$1B_1$ (A') $2A_1$ (A')   (A')
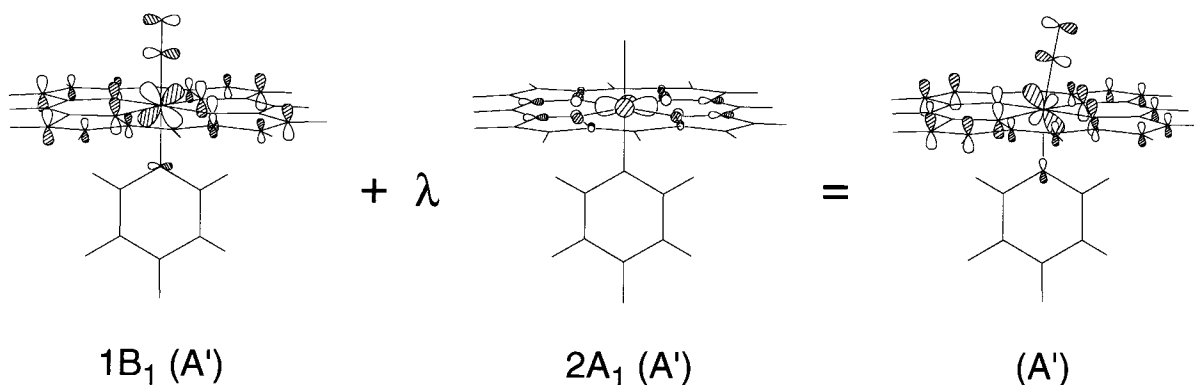
Figure 6. Orbitals $1B_1$ and $2A_1$ in Figure 5 mix upon tilting axial ligands to give the orbital shown on the right.
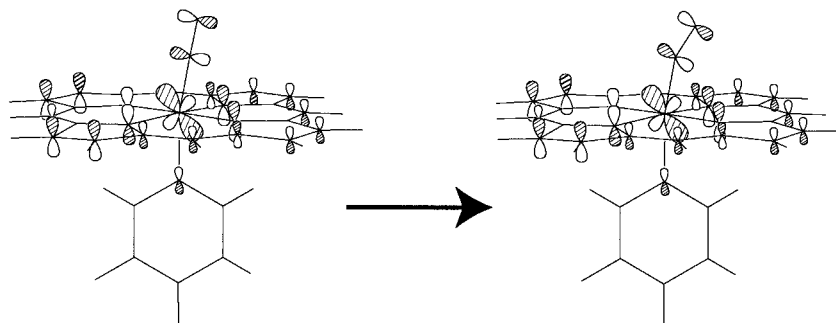
Figure 7. Bending the nitrosyl ligand mixes nitrogen (and oxygen) p_z character into the orbital shown on the left to better align the nodes on the NO π^* and metal d orbitals, as shown on the right.

implies that oxidation of the molecule will result in loss of electron density primarily from the porphyrin ring, rather than the metal.[79] The HOMO is well separated from a LUMO ($2B_2$) and second LUMO ($2B_1$) composed primarily of NO π^* orbitals interacting in an antibonding way with some metal d_{xz} or d_{yz} contributions. The sets $2B_1/2B_2$ and $3B_1/3B_2$ are both antibonding between iron and NO, but differ from each other because the metal−porphyrin π interaction is bonding in the lower-energy $2B_1/2B_2$ set, and antibonding in the $3B_1/3B_2$ pair. The LUMO's composition implies that reduction would result in a slight weakening and lengthening of the Fe−NO bond, but a slight strengthening and shortening of the Fe−N(porphyrin) bonds.

Axial Ligand Tilting and/or Bending. The change in total energy and changes in individual orbital energies upon tilting the p-C_6H_4F and NO ligands off the normal to the porphyrin ring are very small. The total energy surface is relatively flat and shows an increase of only 5 kcal/mol upon tilting the N atom of the NO ligand by 5° (while keeping the FeNO group linear). No large changes in MO energies appear upon tilting the NO ligand off-axis by as much as 10°. Changes in total energy and individual orbital energies, observed upon bending the NO ligand at nitrogen, imply that once the NO ligand tilts off-axis, FeNO prefers to bend away from a perfectly linear geometry. The total energy surface also suggests that increased tilting favors increased bending. Figure S4 shows the change in total energy and changes in individual orbital energies observed upon bending the NO ligand at the nitrogen, once the NO ligand is tilted 6° off-axis.

Although no large orbital energy changes are evident upon tilting the axial ligands, significant orbital mixing occurs. Orbital mixing for axial ligand tilting has already been analyzed in some

detail,[7] and thus we will not repeat the analysis here. The most important feature for our subsequent analysis of ligand bending is the mixing between the orbitals labeled $1B_1$ and $2A_1$ in Figure 5, as shown in Figure 6. The mixing hybridizes the metal contribution to maintain a strong bonding interaction between the metal orbital and the NO π^* contribution to the resulting MO.

Hoffmann, Chen, and Thorn have analyzed orbital energy changes and orbital mixing for ligand bending, but only for geometries in which the bent axial ligands eclipse the equatorial ML bonds.[9] Despite the difference between the geometry analyzed previously and that described here, the analysis of Hoffmann et al. offers key clues to the reasons why FeNO bending *between* the equatorial ligands is energetically favorable, especially *after* tilting the axial ligands. First, a molecular orbital analogous to the metal $d_{x^2-y^2}$ orbital calculated here increases sharply in energy if the axial FeNO group bends to eclipse an equatorial ML bond. This orbital's energy increases because bending the ligand allows an antibonding interaction to develop between the metal $d_{x^2-y^2}$ and NO π^* orbitals.[9] In contrast, when the axial ligand is bent to bisect the N_p−Fe−N_p angle, the nodal plane of the NO π^* orbital coincides with the maximum amplitude of the $d_{x^2-y^2}$ orbital and the two have zero overlap. A second determinant of the large energy barrier for bending an axial ligand along an equatorial M−L bond is the loss of π-bonding between the metal d_{xz} and NO π^* orbitals.[9] If the axial NO ligand is also tilted and is instead bent between the equatorial ligands, the primary effect of NO bending is a mixing of nitrogen (and oxygen) p_z atomic orbitals into the orbital illustrated in Figure 6. The resulting orbital is sketched on the right side of Figure 7 and shows that axial ligand tilting and NO bending effectively conspire to align the nodal surfaces of the metal and nitrosyl contributions to the orbital 3A′ and increase their bonding interaction. Moreover, the energy change of the 3A′ orbital is modulated because its metal d_{xz} component

(79) Electrochemical data for the related (por)Fe(NO)(Ph) (por = TPP, OEP) compounds in PhCN have been reported, but the sites of redox activity were not investigated in detail (ref 41).

**Table 7.** Mössbauer Parameters for Nitrosyl Derivatives at Zero-Applied Field

	ΔE_Q, mm/s	δ_{Fe}, mm/s	T, K	reference
A. {FeNO}^{6} Complexes				
(OEP)Fe(NO)(p-C$_6$H$_4$F)	0.56	0.05	293	this work
	0.57	0.14	4.2	this work
[(OEP)Fe(NO)]ClO$_4$	1.55	0.13	293	59
	1.64	0.20	4.2	59
[(OEP)Fe(NO)]ClO$_4$•CHCl$_3$	1.63	0.12	293	59
	1.65	0.20	4.2	59
[(OEP)Fe(Iz)(NO)]ClO$_4$	1.99	−0.07	293	59
	1.92	0.02	4.2	59
[(OEP)Fe(1-MeIm)(NO)]$^+$ (CH$_3$C(O)N(CH$_3$)$_2$ solution)	1.64	0.02	4.2	97
(TPP)Fe(NO$_2$)(NO)	1.37	0.02	293	50
	1.36	0.13	77	80
	1.36	0.13	4.2	50
(T(p-OCH$_3$)PP)Fe(NO$_2$)(NO)	1.43	0.04	293	50
(TpivPP)Fe(NO$_2$)(NO)	1.48	0.01	293	50
	1.43	0.09	4.2	50
B. {FeNO}^{7} Complexes				
[(TpivPP)Fe(NO$_2$)(NO)]$^-$ (form 2)	1.20	0.35	4.2	81
(TPP)Fe(NO)	1.2	0.35	4.2	81
(OEP)Fe(NO)	1.26	0.35	100	82
C. Fe(II) CO Complexes				
(TPP)Fe(1-MeIm)(CO)	0.35	0.20	293	83
(TPP)Fe(Py)(CO)	0.57	0.28	293	83
(TpivPP)Fe(1-MeIm)(CO)	0.27	0.27	4.2	84
MbCO	0.35	0.27	4.2	85

is distributed over several MOs due to its interaction with the porphyrin π system.

Mössbauer Studies. We have carried out a detailed Mössbauer investigation of (OEP)Fe(NO)(p-C$_6$H$_4$F) in order to study the electronic structure of this highly unusual complex. The Mössbauer spectra demonstrate the purity of the preparations. Importantly, the spectra obtained in an applied magnetic field (Figure S3) also demonstrates the diamagnetic ground state of the complex. The possible nature of the coupling between the iron center and the nitric oxide ligand that leads to an effective diamagnetic state has been discussed recently.[59] The Mössbauer study in applied magnetic field yields the sign (positive) of the quadrupole splitting constant, the value of the asymmetry parameter, the isomer shift δ, and the quadrupole splitting constant ΔE_Q. The underlying diamagnetism unfortunately limits any magnetic information on electronic structure.

The Mössbauer spectrum for (OEP)Fe(NO)(p-C$_6$H$_4$F) is shown in Figure 8. The isomer shift and quadrupole splitting, obtained in zero field, are reported in Table 7 along with all available Mössbauer data for other {FeNO}^{6} porphyrinate derivatives. The data given show that there is wide variation in the Mössbauer parameters of the relatively few {FeNO}^{6} porphyrinate derivatives that have been characterized. Clearly, there is variation in electronic structure as measured by Mössbauer spectroscopy among the group. The species characterized include two crystalline forms of the five-coordinate cation, [(OEP)Fe(NO)]$^+$, which can be considered as the base complex for comparison with all of the other derivatives. Even though the two crystalline forms of the cation have significantly different nitrosyl stretching frequencies, ($\Delta \approx 30$ cm^{-1}), the two forms have very similar Mössbauer parameters in both applied and zero field.

As is well recognized, the iron isomer shift is a measure of the s-electron density at the nucleus and within a closely related set of complexes is also an excellent indicator of the formal charge (oxidation state) of iron.[86,87] The isomer shift for (OEP)-
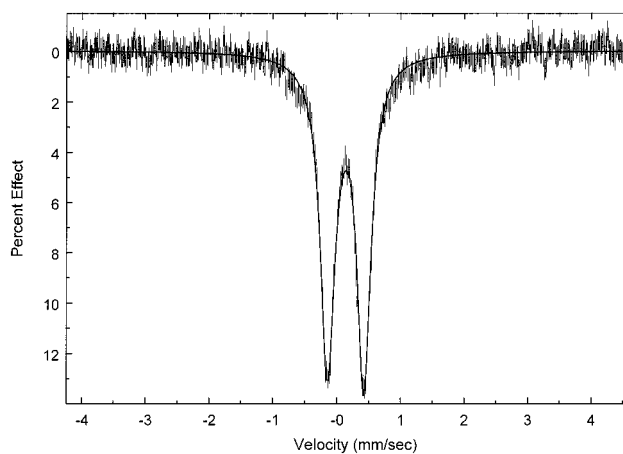
Figure 8. Mössbauer spectrum of (OEP)Fe(NO)(p-C$_6$H$_4$F) in zero applied field at 4.2 K. The solid line is a fit to the data which yields the following parameters: quadrupole splitting $\Delta E_Q = +0.57$ mm/s, isomer shift $\delta = 0.14$ mm/s, and Lorentzian width γ(fwhm) = 0.27 mm/s.

Fe(NO)(p-C$_6$H$_4$F) is within the range of values previously observed for {FeNO}^{6} porphyrinates. All of these {FeNO}^{6} species have isomer shifts smaller than those observed for low-spin iron(III) porphyrinates with two neutral nitrogen donors as the axial ligands.[88−94] We have previously ascribed the lower values of isomer shift in the formally ferric nitrosyl derivatives as the result of strong π-donation from iron to NO rather than an assignment of +4 as the oxidation state of iron.[59] σ-Donation by a sixth ligand is expected to increase the s-density at iron and to lead to a decrease in isomer shift compared to the value observed in the base five-coordinate species. This is indeed observed. The isomer shifts for the species with nitrite, indazole, and imidazole as the sixth ligand are all smaller than those observed for [(OEP)Fe(NO)]$^+$. That the species with nitrite as a sixth ligand has a larger isomer shift (less s-density) than those with imidazole or indazole is unexpected and must represent a net decreased π-donation from iron to NO in the nitrite complex or a net increase in π-accepting at NO in the imidazole and indazole complexes. We believe that the latter is more probable.

(80) Settin, M. F.; Fanning, J. C. *Inorg. Chem.* **1988**, *27*, 1431−1435.

(81) Nasri, H.; Ellison, M. K.; Chen, S.; Huynh, B. H.; Scheidt, W. R. *J. Am. Chem. Soc.* **1997**, *119*, 6274−6283.

(82) Bohle, D. S.; Debrunner, P.; Fitzgerald, J. P.; Hansert, B.; Hung, C.-H.; Thomson, A. J. *Chem. Commun.* **1997**, 91−92.

(83) Havlin, R. H.; Godbout, N.; Salzmann, R.; Wojdelski, M.; Arnold, W.; Schulz, C. E.; Oldfield, E. *J. Am. Chem. Soc.* **1998**, *120*, 3144−3151.

(84) Collman, J. P.; Gagne, R. R.; Halbert, T. R.; Lang, G.; Robinson, W. T. *J. Am. Chem. Soc.* **1975**, *97*, 1427−1439.

(85) Maeda, Y.; Harami, T.; Morita, Y.; Trautwein, A. X.; Gonser, U. *J. Chem. Phys.* **1981**, *75*, 36−43.

(86) Debrunner, P. G. In *Iron Porphyrins, Part 3*; Lever, A. B. P., Gray, H. B., Eds.; VCH Publishers Inc.: New York, 1983; Chapter 2.

(87) Wolff, T. E.; Berg, J. M.; Hodgson, K. O.; Frankel, R. B.; Holm, R. H. *J. Am. Chem. Soc.* **1979**, *101*, 4140−4150.

(88) Safo, M. K.; Gupta, G. P.; Watson, C. T.; Simonis, U.; Walker, F. A.; Scheidt, W. R. *J. Am. Chem. Soc.* **1992**, *114*, 7066−7075.

(89) Safo, M. K.; Gupta, G. P.; Walker, F. A.; Scheidt, W. R. *J. Am. Chem. Soc.* **1991**, *113*, 5497−5510.

(90) Munro, O. Q.; Marques, H. M.; Debrunner, P. G.; Mohanrao, K.; Scheidt, W. R. *J. Am. Chem. Soc.* **1995**, *117*, 935−954.

(91) Safo, M. K.; Walker, F. A.; Raitsimring, A. M.; Walters, W. P.; Dolata, D. P.; Debrunner, P. G.; Scheidt, W. R. *J. Am. Chem. Soc.* **1994**, *116*, 7760−7770.

(92) (a) Epstein, L. M.; Straub, D. K.; Mariconi, C. *Inorg. Chem.* **1967**, *6*, 1720−1724. (b) Inniss, D.; Soltis, S. M.; Strouse, C. E. *J. Am. Chem. Soc.* **1988**, *110*, 5644−5650.

(93) Scheidt, W. R.; Osvath, S. R.; Lee, Y. J.; Reed, C. A.; Shaevitz, B.; Gupta, G. P. *Inorg. Chem.* **1989**, *28*, 1591−1595.

(94) Straub, D. K.; Conner, W. M. *Ann. N.Y. Acad. Sci.* **1973**, *206*, 383−395.

The strongly σ-donating aryl ligand in (OEP)Fe(NO)(p-C$_6$H$_4$F) would be expected to lead to the smallest value of isomer shift. That this difference is not observed must result from decreased π-donation from iron to NO. In this σ-aryl complex the decreased π-bonding is clearly reflected in the structure of the bent Fe−N−O group.

The quadrupole splitting constant for (OEP)Fe(NO)(p-C$_6$H$_4$F) of +0.57 mm/s is much smaller than any of the other nitrosyl species and indeed is much smaller than any low-spin iron(III) porphyrinate.[86] The very low value of the quadrupole splitting suggests that the anisotropy in the iron 3d shell is small. Given the ground-state diamagnetism of these {FeNO}⁶ complexes, an analysis of the quadrupole splitting constant variation in terms of a low-spin d⁶ electronic configuration appears to be warranted. The quadrupole splitting constant (ΔE_Q) is related to the electric field gradient tensor (EFG) at the nucleus by the following equation:

$$\Delta E_Q = \frac{1}{2} eQV_{zz}\left(1 + \frac{\eta^2}{3}\right)^{1/2}$$

where e is the electron charge, Q is the quadrupole moment, and V_{zz} is the largest component of the EFG tensor and

$$\eta = \frac{V_{xx} - V_{yy}}{V_{zz}}$$

The principal components of the EFG satisfy $|V_{zz}| > |V_{yy}| > |V_{xx}|$. The experimentally determined asymmetry parameter, η, in these complexes is zero within the experimental uncertainty. When the asymmetry parameter is zero, the EFG can be restricted to the V_{zz} component. The contributions to V_{zz} can be restricted to valence, covalence, and ligand contributions, with the valence and covalence contributions expected to dominate. The anisotropy of the iron 3d shell can be expressed by the following:[95]

$$\Delta n_d = n(d_{x^2-y^2}) + n(d_{xy}) - n(d_{z^2}) - \frac{n(d_{xz}) + n(d_{yz})}{2}$$

Differences in the observed quadrupole splitting parameters in the {FeNO}⁶ species should be reflected by the differing anisotropy of the valence shell occupation Δn_d. Changes in the anisotropy of the valence shell will be determined by the σ-donor and π-accepting capabilities of the two axial ligands. From our data for {FeNO}⁶ species, this must include variation in the π-bonding interaction between iron and NO. The low quadrupole splitting constant in the present aryl complex is consistent with the strong σ-donating ability of the aryl anion. This, and the weakened π-accepting capability of NO, both serve to decrease the value of ΔE_Q. The difference in ΔE_Q for the nitrite complex (decreased) and the indazole complex (increased) compared to the five-coordinate reference species must be due to differences in the Fe−NO π-bonding; increased π-acceptance in the indazole derivative and decreased π-acceptance in the nitrite species. That the imidazole complex has a quadrupole splitting constant similar to that of the five-coordinate species must reflect the combination of the σ-donation and modest π-donor ability of imidazole along with increased π-donation from iron to NO. These Fe−N−O π-bonding differences are totally consistent with the isomer shift data considered earlier. The Mössbauer data thus strongly support the idea that the sixth ligand, trans to NO, has a significant effect on the Fe−N−O π-bonding. The

least σ-basic ligand, indazole, leads to the strongest Fe−N−O π-bonding, while the most σ-basic ligand, p-fluorophenyl, leads to the weakest Fe−N−O π-bonding.

Interestingly, this variation in Fe−N−O π-bonding is not exactly suggested by the pattern of the nitrosyl stretching frequency changes, which are commonly thought to be due to differences in Fe to NO π-back-donation and where the indazole species has the highest υ_{NO} at 1914 cm^{-1}. The observation that υ_{NO} of the five-coordinate {FeNO}⁶ species is in the middle of the range of six-coordinate {FeNO}⁶ species is unexpected and suggests subtle effects on the nitrosyl stretching frequency. However, the differences in υ_{NO} follow the observed differences in Fe−N−O angle, although the experimental X-ray data are somewhat hampered by crystallographic disorder problems for many of the nitro(nitrosyl) derivatives. The indazole and related derivatives have effectively linear Fe−N−O groups; the nitro-(nitrosyls) appear to have Fe−N−O groups bent by approximately 10°, while the aryl species has the strongly bent Fe−N−O group. The sequence of decreasing υ_{NO} follows the observed variation in the bending of Fe−N−O. A theoretical evaluation of possible contributions to the Mössbauer spectra and a comparison of calculated values of the asymmetry parameter, η, and quadrupole splitting parameter, ΔE_Q, would be desirable but are beyond the scope of this investigation. See for example Havlin et al.[83] for an example of such detailed theoretical calculations.

Concluding Remarks

We have prepared and structurally characterized the very unusual Fe and Ru compounds (OEP)M(NO)(p-C$_6$H$_4$F). The observation of significantly bent M−N−O groups in these {MNO}⁶ species is unprecedented. The current dogma that assigns a linear MNO linkage in ferric nitrosyl hemes has to be modified to include the possibility of low-energy bending coupled with axial tilting of the FeNO group. Bent Fe−N−O linkages are now seen to be possible for both formally ferrous and ferric nitrosyl porphyrins. The bending of the M−N−O group seen in (OEP)M(NO)(p-C$_6$H$_4$F) appears intrinsic to species of the type (por)M(NO)X when X is a strong σ-donor ligand. Indeed, Mössbauer data for several {FeNO}⁶ species show that the sixth ligand has a significant effect on the Fe−NO π-bonding. Our results also suggest that related classes of compounds of the type (por)M(NO)X could also display similar axial NO tilting/bending features.[96,97] Further studies to investigate the effect of the trans axial ligand on this tilting/bending feature of NO ligands are in progress. Quantum calculations show that the unexpected bending of the FeNO group coupled with axial FeNO tilting is due to electronic factors. Specifically, hybrid Hartree−Fock/density functional calculations for (porph)-Fe(NO)(p-C$_6$H$_4$F) show that a structure with both the p-C$_6$H$_4$F and NO ligands tilted off-axis and the FeNO group bent is a minimum-energy structure. These calculations approximately reproduce the observed tilt angles, extent of FeNO bending, and the N−O, Fe−NO, and Fe−N$_p$ bond distances in the parent (OEP)Fe(NO)(p-C$_6$H$_4$F) compound. Extended Hückel calculations show that bending the FeNO group to bisect a N$_p$−Fe−N$_p$ angle gives a lower energy barrier than bending in a direction eclipsing an equatorial Fe−N$_p$ bond because overlap between the NO π^* orbital and the metal d$_{x^2-y^2}$ orbital is zero.

(95) Paulsen, H.; Kröckel, M.; Grodzicki, M.; Bill, E.; Trautwein, A. X.; Leigh, G. J.; Silver, J. *Inorg. Chem.* 1995, *34*, 6244−6249.

(96) We have also very recently observed axial NO tilting and bending in the crystal structure of the related (OEP)Os(NO)(OEt) complex: Cheng, L.; Powell, D. R.; Khan, M. A.; Richter-Addo, G. B. *Inorg. Chem.* 2001, *40*, 125−133

(97) Schünemann, V.; Benda, R.; Trautwein, A. X.; Walker, F. A. *Isr. J. Chem.* 2000, *40*, 9.

Supporting Information Available: Tables S1−S6, giving complete crystallographic details, atomic coordinates, bond distances and angles, anisotropic temperature factors, and fixed hydrogen atom positions for (OEP)Fe(NO)(p-C$_6$H$_4$F); Tables S7−S16, giving complete crystallographic details, atomic coordinates, bond distances and angles, anisotropic temperature factors, and fixed hydrogen atom positions for (OEP)Ru(NO)-(p-C$_6$H$_4$F) at the two temperatures; Table S17 giving extended Hückel parameters used in this work; Figures S1 and S2 showing the closest intermolecular contacts with the nitrosyl group in (OEP)Ru(NO)(p-C$_6$H$_4$F) and (TTP)Ru(NO)(p-C$_6$H$_4$F), respectively; Figure S3 showing the Mössbauer spectrum of (OEP)-Fe(NO)(p-C$_6$H$_4$F) in an applied magnetic field at 4.2 K; Figure S4 presenting a Walsh diagram indicating changes in individual orbital energies for (porph)Fe(NO)(p-C$_6$H$_4$F) upon bending the NO ligand (PDF). X-ray crystallographic files, in CIF format. This material is available free of charge via the Internet at http://pubs.acs.org.

JA010276M